

# Vector Precoding for Wireless MIMO Systems: A Replica Analysis

Ralf R. Müller, Dongning Guo, and Aris L. Moustakas

## Abstract

We apply the replica method to analyze vector precoding, a method to reduce transmit power in antenna array communications. The analysis applies to a very general class of channel matrices. The statistics of the channel matrix enter the transmitted energy per symbol via its R-transform. We find that vector precoding performs much better for complex than for real alphabets.

As a byproduct, we find a nonlinear precoding method with polynomial complexity that outperforms NP-hard Tomlinson-Harashima precoding for binary modulation on complex channels if the number of transmit antennas is slightly larger than twice the number of receive antennas.

## I. INTRODUCTION

Wireless multiple-input multiple-output (MIMO) systems offer the possibility to increase data rate over conventional wireless communications without need for more physical radio spectrum by means of multiple antenna elements at both transmitter and receiver side. Since the pioneering work in the field [5], [18], countless implementations for those MIMO systems have been proposed. They can be classified by the side where the signal processing takes place. Depending on the proposed system solution, there can be need for major signal processing at the receiver side, the transmitter side or both of them. This work is concerned with systems where sophisticated signal processing is required solely at the transmitter side. This is advantageous for transmitting data to low-cost or battery-driven devices such as cell-phones and PDAs.

It is an unavoidable feature of wireless MIMO systems that signals sent at different antenna elements of the transmit array are received with severe crosstalk at the respective antenna elements of the receive array. In order to compensate for this crosstalk, one can use linear joint transmitter processing, also known as linear vector precoding, as suggested in [22], [16]. This comes, however, at the expense of the need for an increased transmit power in order to maintain the distance properties of the signal constellation. A more sophisticated method for transmitter processing is nonlinear vector precoding, in this work simply referred to as vector precoding. It is based on the concept of Tomlinson-Harashima precoding [19], [7] which was originally proposed to combat intersymbol interference. It was proposed for use in context of MIMO systems in [23], [9]. For a general survey on vector precoding the reader is referred to [4].

In this work, we are mainly concerned with the performance analysis of vector precoding. To the best of our knowledge, there is no published literature on the performance analysis of nonlinear vector precoding by analytical means. This paper aims to pave the way a first step forward towards this direction employing the replica method which was originally invented for the analysis of spin glasses in statistical physics [13], [3] and has become increasingly powerful to address problems in wireless communications and coding theory [14]. We use the analytical results developed in this paper to compare real-valued vector precoding with complex-valued vector precoding as well as with some hybrid forms of it which are newly proposed in this work.

R. Müller is with the Department of Electronics and Telecommunications, The Norwegian University of Science and Technology, Trondheim, Norway, e-mail:ralf@iet.ntnu.no

D. Guo is with the Department of Electrical Engineering and Computer Science, Northwestern University, Evanston, IL, USA, e-mail:dGuo@northwestern.edu

A. Moustakas is with the Physics Department, National and Kapodistrian University of Athens, Athens, Greece, e-mail:arism@phys.uoa.gr

The paper is composed of five more sections. Section II introduces vector precoding from a general point of view. This point of view is more general than the way vector precoding is dealt with in the references mentioned earlier, but it is well suited to the replica analysis to follow. Section III formulates vector precoding as a non-convex quadratic programming problem and introduces the technical assumptions that we require for the analytical analysis. Section IV derives the general replica symmetric solution to any non-convex quadratic programming problem for which the search space can be factorized into Kronecker products of scalar sets in the limit of a large number of dimensions of the search space. Section V specializes the general results to MIMO channels with channel matrices composed of independent identically distributed entries and various choices for the relaxation of the symbol alphabet. Section VI summarizes the main conclusions. Particularly technical derivations are placed in the two appendices.

## II. VECTOR PRECODING

Vector precoding aims to minimize the transmitted power that is associated with the transmission of a certain data vector  $\mathbf{s} \in \mathcal{S}^K$  of length  $K$ . For that purpose, the original symbol alphabet  $\mathcal{S}$  is relaxed into the alphabet  $\mathcal{B}$ . The data representation in the relaxed alphabet is redundant. That means that several symbols in the relaxed alphabet represent the same data. Due to the redundant representation, we can now choose that representation of our data which requires the least power to be transmitted. This way of saving transmit power is what we call vector precoding.

That means, for any  $s \in \mathcal{S}$  there is a set  $\mathcal{B}_s \subset \mathcal{B}$  such that all elements of  $\mathcal{B}_s$  represent the data  $s$ . Take binary transmission as an example, i.e.  $\mathcal{S} = \{1, 0\}$ . Without vector precoding, it is most common to choose  $\mathcal{B}_0 = \{+1\}$  and  $\mathcal{B}_1 = \{-1\}$ . This modulation is called binary phase shift keying. For binary modulation, vector precoding is the idea to have  $\mathcal{B}_0 \supset \{+1\}$  and  $\mathcal{B}_1 \supset \{-1\}$ , i.e. to allow for supersets of the binary constellation. A popular choice for those supersets is due to Tomlinson and Harashima [19], [7], see also Fig. 1. Here, we have  $\mathcal{B}_0 = 4\mathbb{Z} + 1$  and  $\mathcal{B}_1 = 4\mathbb{Z} - 1$ .

In order to avoid ambiguities, we should have

$$\mathcal{B}_i \cap \mathcal{B}_j = \emptyset \quad \forall i \neq j. \quad (1)$$

In addition, one would like to design the sets  $\mathcal{B}_i$  such that the distance properties between the presented information are preserved. This is easily achieved by letting the sets  $\mathcal{B}_i$  to be distinct sub-lattices of  $\mathcal{B}$ . However, we are not concerned with these design issues here. We aim to analyze the power saving achieved by a particular choice of the sets  $\mathcal{B}_i$ . This goal is achieved using the replica method invented in statistical physics.

## III. PROBLEM STATEMENT

Let  $\mathbf{s} = [s_1, \dots, s_K]^T$  denote the information to be encoded. Let  $\mathbf{t} = \mathbf{T}\mathbf{x}$  be the vector being sent. Then, the precoding problem can be written as the minimization of the following quadratic form

$$\min_{\mathbf{x} \in \mathcal{X}} \|\mathbf{T}\mathbf{x}\|^2 = \min_{\mathbf{x} \in \mathcal{X}} \mathbf{x}^\dagger \mathbf{J} \mathbf{x} \quad (2)$$

over the discrete set

$$\mathcal{X} = \mathcal{B}_{s_1} \times \mathcal{B}_{s_2} \times \dots \times \mathcal{B}_{s_K} \quad (3)$$

with  $\mathbf{J} = \mathbf{T}^\dagger \mathbf{T}$ . This type of problem is known in context of optimization as non-convex quadratic programming.

In order to allow for analytical tractability, we need the following definition and assumptions:

**DEFINITION 1 (R-TRANSFORM)** *Let  $P(x)$  denote an arbitrary probability distribution. Let*

$$m(s) = \int \frac{dP(x)}{x - s}. \quad (4)$$

Then, the  $R$ -transform of  $P(x)$  is

$$R(w) = m^{-1}(-w) - \frac{1}{w} \quad (5)$$

with  $m^{-1}(w)$  denoting the inverse of  $m(s)$  with respect to composition, i.e.  $m^{-1}(m(s)) = s$ .

ASSUMPTION 1 (SELF-AVERAGING PROPERTY) We have

$$\lim_{K \rightarrow \infty} \Pr \left( \frac{1}{K} \left| \min_{\mathbf{x} \in \mathcal{X}} \mathbf{x}^\dagger \mathbf{J} \mathbf{x} - \mathbb{E}_{\mathbf{J}} \min_{\mathbf{x} \in \mathcal{X}} \mathbf{x}^\dagger \mathbf{J} \mathbf{x} \right| > \epsilon \right) = 0 \quad (6)$$

for all  $\epsilon > 0$ , i.e. convergence in probability.

ASSUMPTION 2 (REPLICA CONTINUITY) For all  $\beta > 0$ , the continuation of the function

$$f(n) = \prod_{a=1}^n \sum_{\mathbf{x}_a \in \mathcal{X}} e^{-\beta \mathbf{x}_a^\dagger \mathbf{J} \mathbf{x}_a} \quad (7)$$

onto the positive real line is equal to

$$\left( \sum_{\mathbf{x} \in \mathcal{X}} e^{-\beta \mathbf{x}^\dagger \mathbf{J} \mathbf{x}} \right)^n$$

in the right-sided vicinity of  $n = 0$ .

ASSUMPTION 3 (UNITARY INVARIANCE) The random matrix  $\mathbf{J}$ , can be decomposed into

$$\mathbf{J} = \mathbf{O} \mathbf{D} \mathbf{O}^\dagger \quad (8)$$

such that the matrices  $\mathbf{D}$  and  $\mathbf{O}$  are diagonal and Haar distributed, respectively. Moreover, as  $K \rightarrow \infty$ , the asymptotic eigenvalue distribution of  $\mathbf{J}$  converges to a non-random distribution function which can be uniquely characterized by its  $R$ -transform  $R(w)$ .

ASSUMPTION 4 (REPLICA SYMMETRY) When applying the replica method to solve the saddle-point equations, we will assume that the extremal point is invariant to permutations of the replica index. For a detailed discussion of replica symmetry, the reader is referred to the literature of spin glasses, e.g. [13], [3].

The first three assumptions are rather technical and should hold well in the application we are addressing. The validity of replica symmetry for the minimum value of  $\mathbf{x}^\dagger \mathbf{J} \mathbf{x}$  is an approximation, which is made for analytical tractability and, for sake of simplicity, no further justification is made here. It should be pointed out though that, even when replica symmetry is not valid the correct value of quantities such as  $E_s$  do not differ much from the corresponding values evaluated within the replica-symmetric assumption, cf. [11], [12].

#### IV. GENERAL RESULT

In this section, we derive a general solution to the non-convex quadratic programming problem (2) in the limit of a large number of dimensions  $K$ . We find the following result:

PROPOSITION 1 Let Assumptions 1 to 4 hold. Let  $P_s(s)$  denote the limit of the empirical distribution function of the information symbols  $s_1, \dots, s_K$  as  $K \rightarrow \infty$ . Moreover, let the parameters  $q$  and  $b$  be solutions to the following pair of coupled fixed-point equations

$$q = \iint \left| \operatorname{argmin}_{x \in \mathcal{B}_s} \left| z \sqrt{\frac{qR'(-b)}{2R^2(-b)}} - x \right| \right|^2 \mathrm{D}z \mathrm{d}P_s(s) \quad (9)$$

$$b = \iint \Re \left\{ \operatorname{argmin}_{x \in \mathcal{B}_s} \left| z \sqrt{\frac{qR'(-b)}{2R^2(-b)}} - x \right| z^* \right\} \frac{\mathrm{D}z \mathrm{d}P_s(s)}{\sqrt{2qR'(-b)}}. \quad (10)$$

with  $Dz = \exp(-z^2/2)/(2\pi)dz$  being the complex Gaussian measure. Then, if  $0 < b < \infty$ , we have

$$\frac{1}{K} \min_{\mathbf{x} \in \mathcal{X}} \mathbf{x}^\dagger \mathbf{J} \mathbf{x} \rightarrow q \frac{\partial}{\partial b} bR(-b) \quad (11)$$

in probability as  $K \rightarrow \infty$ .

The remainder of this section is dedicated to the derivation of Proposition 1. Further sections will not make reference to the remainder of Section IV.

With Assumptions 1 and 2, we find for the average transmitted energy per symbol in the large system limit

$$E_s = \lim_{K \rightarrow \infty} \frac{1}{K} \min_{\mathbf{x} \in \mathcal{X}} \mathbf{x}^\dagger \mathbf{J} \mathbf{x} \quad (12)$$

$$= - \lim_{K \rightarrow \infty} \lim_{\beta \rightarrow \infty} \frac{1}{\beta K} \mathbb{E}_{\mathbf{J}} \log \sum_{\mathbf{x} \in \mathcal{X}} e^{-\beta \mathbf{x}^\dagger \mathbf{J} \mathbf{x}} \quad (13)$$

$$= - \lim_{K \rightarrow \infty} \lim_{\beta \rightarrow \infty} \frac{1}{\beta K} \lim_{n \rightarrow 0} \frac{\partial}{\partial n} \log \mathbb{E}_{\mathbf{J}} \left( \sum_{\mathbf{x} \in \mathcal{X}} e^{-\beta \mathbf{x}^\dagger \mathbf{J} \mathbf{x}} \right)^n \quad (14)$$

$$= - \lim_{\beta \rightarrow \infty} \frac{1}{\beta} \lim_{n \rightarrow 0} \frac{\partial}{\partial n} \underbrace{\lim_{K \rightarrow \infty} \frac{1}{K} \log \mathbb{E}_{\mathbf{J}} \prod_{a=1}^n \sum_{\mathbf{x}_a \in \mathcal{X}} e^{-\beta \mathbf{x}_a^\dagger \mathbf{J} \mathbf{x}_a}}_{\triangleq \Xi_n}.$$

where the argument of the logarithm in (15) is given by<sup>1</sup>

$$\begin{aligned} \Xi_n &= \lim_{K \rightarrow \infty} \frac{1}{K} \log \mathbb{E}_{\mathbf{J}} \sum_{\{\mathbf{x}_a \in \mathcal{X}\}} \exp \left[ -\beta \sum_{a=1}^n \mathbf{x}_a^\dagger \mathbf{J} \mathbf{x}_a \right] \\ &= \lim_{K \rightarrow \infty} \frac{1}{K} \log \mathbb{E}_{\mathbf{J}} \sum_{\{\mathbf{x}_a \in \mathcal{X}\}} \exp \left[ \text{tr} \left( -\beta \mathbf{J} \sum_{a=1}^n \mathbf{x}_a \mathbf{x}_a^\dagger \right) \right]. \end{aligned} \quad (15)$$

Using Assumption 3, we can integrate over the Haar distributed eigenvectors of  $\mathbf{J}$ . This integration was studied by Harish-Chandra [8] and Itzykson & Zuber [10] in the mathematics and physics literature, respectively. It was applied in context of wireless communications in [17]. Guionnet and Maïda [6] solve this integral in terms of the R-transform  $R(w)$  of the asymptotic eigenvalue distribution of  $\mathbf{J}$ . Following their approach yields

$$\Xi_n = \lim_{K \rightarrow \infty} \frac{1}{K} \log \sum_{\{\mathbf{x}_a \in \mathcal{X}\}} \exp \left[ -K \sum_{a=1}^n \int_0^{\lambda_a} R(-w) dw \right] \quad (16)$$

with  $\lambda_i$  denoting the  $n$  positive eigenvalues of

$$\beta \sum_{a=1}^n \mathbf{x}_a \mathbf{x}_a^\dagger. \quad (17)$$

The eigenvalues  $\lambda_i$  are completely determined by the inner products

$$KQ_{ab} = \mathbf{x}_a^\dagger \mathbf{x}_b \triangleq \sum_{k=1}^K x_{ak}^* x_{bk}. \quad (18)$$

<sup>1</sup>The notation  $\sum_{\{x_a\}}$  is used as shortcut for  $\sum_{x_1} \sum_{x_2} \cdots \sum_{x_n}$ .

In order to perform the summation in (16), the  $Kn$ -dimensional space spanned by the replicas is split into subshells

$$S\{Q\} \triangleq \{\mathbf{x}_1, \dots, \mathbf{x}_n \mid \mathbf{x}_a^\dagger \mathbf{x}_b = KQ_{ab}\} \quad (19)$$

where the inner product of two different replicated vectors  $\mathbf{x}_a$  and  $\mathbf{x}_b$  is constant in each subshell.<sup>2</sup> With this splitting of the space, we find<sup>3</sup>

$$\Xi_n = \lim_{K \rightarrow \infty} \frac{1}{K} \log \int_{\mathbb{C}^{n^2}} e^{K\mathcal{I}\{Q\}} e^{-K\mathcal{G}\{Q\}} \prod_{a,b} dQ_{ab}, \quad (20)$$

where

$$\mathcal{G}\{Q\} = \sum_{a=1}^n \int_0^{\lambda_a\{Q\}} R(-w) dw \quad (21)$$

and

$$e^{K\mathcal{I}\{Q\}} = \sum_{\{\mathbf{x}_a \in \mathcal{X}\}} \prod_{a,b} \delta(\mathbf{x}_a^\dagger \mathbf{x}_b - KQ_{ab}) \quad (22)$$

denotes the probability weight of the subshell composed of two-dimensional Dirac-functions in the complex plane. This procedure is a change of integration variables in multiple dimensions where the integration of an exponential function over the replicas has been replaced by integration over the variables  $\{Q\}$ . In the following the two exponential terms in (20) are evaluated separately.

First, we turn to the evaluation of the measure  $e^{K\mathcal{I}\{Q\}}$ . The Fourier expansion of the Dirac measure

$$\delta(\mathbf{x}_a^\dagger \mathbf{x}_b - KQ_{ab}) = \int_{\mathcal{J}} \exp\left[\tilde{Q}_{ab}(\mathbf{x}_a^\dagger \mathbf{x}_b - KQ_{ab})\right] \frac{d\tilde{Q}_{ab}}{2\pi j} \quad (23)$$

with  $\mathcal{J} = (t - j\infty; t + j\infty)$ , gives

$$e^{K\mathcal{I}\{Q\}} = \sum_{\{\mathbf{x}_a \in \mathcal{X}\}} \prod_{a,b} \int_{\mathcal{J}} e^{\tilde{Q}_{ab}(\mathbf{x}_a^\dagger \mathbf{x}_b - KQ_{ab})} \frac{d\tilde{Q}_{ab}}{2\pi j} \quad (24)$$

$$= \int_{\mathcal{J}^{n^2}} e^{\log \prod_{k=1}^K M_k\{\tilde{Q}\} - K \sum_{a,b} \tilde{Q}_{ab} Q_{ab}} \prod_{a,b} \frac{d\tilde{Q}_{ab}}{2\pi j} \quad (25)$$

with

$$M_k\{\tilde{Q}\} = \sum_{\{\mathbf{x}_a \in \mathcal{B}_{s_k}\}} e^{\sum_{a,b} \tilde{Q}_{ab} \mathbf{x}_a^* \mathbf{x}_b}. \quad (26)$$

In the limit of  $K \rightarrow \infty$  one of the exponential terms in (20) will dominate over all others. Thus, only the maximum value of the correlation  $Q_{ab}$  is relevant for calculation of the integral.

At this point, we assume replica symmetry. This means, that in order to find the maximum of the objective function, we consider only a subset of the potential possibilities that the variables  $Q_{ab}$  could take. In particular, we are interested in the most general form of the positive semidefinite matrix  $\mathbf{Q}$  with permutational symmetry when exchanging its replica indices. Therefore, we need a matrix with all off-diagonal elements equal to each other. Thus, we restrict them to the following two different possibilities  $Q_{ab} = q, \forall a \neq b$  and  $Q_{aa} = q + b/\beta, \forall a$  where  $b \geq 0$  since  $\mathbf{Q}$  has to be positive semidefinite. One case distinction has been made to distinguish correlations  $Q_{ab}$  which correspond to correlations between

<sup>2</sup>The notation  $f\{Q\}$  expresses dependency of the function  $f(\cdot)$  on  $Q_{ab} \forall a, b$ .

<sup>3</sup>The notation  $\prod_{a,b}$  is used as shortcut for  $\prod_{a=1}^n \prod_{b=1}^n$ .

different and identical replica indices, respectively. We apply the same idea to the correlation variables in the dual (Fourier) domain and set with a modest amount of foresight  $\tilde{Q}_{ab} = \beta^2 f^2/2, \forall a \neq b$  and  $\tilde{Q}_{aa} = \beta^2 f^2/2 - \beta e, \forall a$ . Note that despite the fact that  $\mathbf{Q}$  is complex, in general, its values at the saddle-point are in fact real.

At this point the crucial benefit of the replica method becomes obvious. Assuming replica continuity, we have managed to reduce the evaluation of a continuous function to sampling it at integer points. Assuming replica symmetry we have reduced the task of evaluating infinitely many integer points to calculating four different correlations (two in the original and two in the Fourier domain).

The assumption of replica symmetry leads to

$$\sum_{a,b} \tilde{Q}_{ab} Q_{ab} = \frac{n(n-1)}{2} \beta^2 f^2 q + n \left( \frac{\beta f^2}{2} - e \right) (\beta q + b) \quad (27)$$

and

$$M_k(e, f) = \sum_{\{x_a \in \mathcal{B}_{s_k}\}} e^{\frac{\beta}{2} \sum_{a=1}^n (\beta f^2 - 2e) |x_a|^2 + 2 \sum_{b=a+1}^n \beta f^2 \Re\{x_a^* x_b\}} \quad (28)$$

Note that the prior distribution enters the free energy only via (28). We will focus on this later on after having finished with the other terms.

For the evaluation of  $\mathcal{G}\{Q\}$  in (20), we can use the replica symmetry to explicitly calculate the eigenvalues  $\lambda_i$ . Considerations of linear algebra lead to the conclusion that the eigenvalues  $b$  and  $b + \beta n q$  occur with multiplicities  $n - 1$  and  $1$ , respectively. Thus we get

$$\mathcal{G}(q, b) = (n-1) \int_0^b R(-w) dw + \int_0^{b+\beta n q} R(-w) dw. \quad (29)$$

Since the integral in (20) is dominated by the maximum argument of the exponential function, the derivatives of

$$\mathcal{G}\{Q\} + \sum_{a,b} \tilde{Q}_{ab} Q_{ab} \quad (30)$$

with respect to  $q$  and  $b$  must vanish as  $K \rightarrow \infty$ .<sup>4</sup> Taking derivatives after plugging (27) and (29) into (30), gives

$$\begin{aligned} \beta n R(-b - \beta n q) + \frac{n(n-1)}{2} \beta^2 f^2 + \beta n \left( \frac{\beta f^2}{2} - e \right) &= 0 \\ (n-1) R(-b) + R(-b - \beta n q) + n \left( \frac{\beta f^2}{2} - e \right) &= 0 \end{aligned}$$

solving for  $e$  and  $f$  gives

$$e = R(-b) \quad (31)$$

$$f = \sqrt{2 \frac{R(-b) - R(-b - \beta n q)}{\beta n}} \quad (32)$$

with the limits for  $n \rightarrow 0$

$$f \xrightarrow{n \rightarrow 0} \sqrt{2q R'(-b)} \quad (33)$$

$$n \frac{\partial f}{\partial n} \xrightarrow{n \rightarrow 0} 0. \quad (34)$$

<sup>4</sup> It turns out that when  $\lim_{n \rightarrow 0} \partial_n \Xi_n$  is expressed in terms of  $e, f, q, b$ , the relevant extremum is in fact a maximum and not a minimum. This is due to the fact that when drops below unity, the minima of a function become maxima and vice-versa. For a detailed analysis of this technicality, see [15].

Consider now the integration over the prior distribution in the moment-generating function. Consider (28) giving the only term that involves the prior distribution and apply the complex Hubbard-Stratonovich transform

$$e^{-\frac{|z|^2}{2}} = \frac{1}{2\pi} \int_{\mathbb{C}} e^{\Re\{xz^*\} - \frac{|z|^2}{2}} dz = \int e^{\Re\{xz\}} Dz. \quad (35)$$

Then, we find with (28)

$$M_k(e, f) = \sum_{\{x_a \in \mathcal{B}_{s_k}\}} e^{\frac{\beta^2 f^2}{2} \left| \sum_{a=1}^n x_a \right|^2 - \sum_{a=1}^n \beta e |x_a|^2} \quad (36)$$

$$= \sum_{\{x_a \in \mathcal{B}_{s_k}\}} \int e^{\beta \sum_{a=1}^n f \Re\{x_a z^*\} - e |x_a|^2} Dz \quad (37)$$

$$= \int \left( \sum_{x \in \mathcal{B}_{s_k}} e^{\beta f \Re\{xz^*\} - \beta e |x|^2} \right)^n Dz \quad (38)$$

Moreover, for  $K \rightarrow \infty$ , we have by the law of large numbers

$$\begin{aligned} \log M(e, f) &= \frac{1}{K} \log \prod_{k=1}^K M_k(e, f) \\ &\rightarrow \int \log \int \left( \sum_{x \in \mathcal{B}_s} e^{\beta f \Re\{z^*x\} - \beta e |x|^2} \right)^n Dz dP_s(s). \end{aligned} \quad (39)$$

In the large system limit, the integral in (25) is dominated by that value of the integration variable which maximizes the argument of the exponential function. Thus, partial derivatives of

$$\log M(e, f) - \frac{n(n-1)}{2} f^2 \beta^2 q - n \left( \frac{\beta f^2}{2} - e \right) (b + \beta q) \quad (40)$$

with respect to  $f$  and  $e$  must vanish as  $K \rightarrow \infty$ .

An explicit calculation of the two derivatives gives the following expressions for the macroscopic parameters  $q$  and  $b$

$$b = \frac{1}{\sqrt{2qR'(-b)}} \iint \frac{\sum_{x \in \mathcal{B}_s} \Re\{z^*x\} e^{\beta \sqrt{2qR'(-b)} \Re\{z^*x\} - \beta R(-b)|x|^2}}{\sum_{x \in \mathcal{B}_s} e^{\beta \sqrt{2qR'(-b)} \Re\{z^*x\} - \beta R(-b)|x|^2}} Dz dP_s(s) \quad (41)$$

$$q = \iint \frac{\sum_{x \in \mathcal{B}_s} |x|^2 e^{\beta \sqrt{2qR'(-b)} \Re\{z^*x\} - \beta R(-b)|x|^2}}{\sum_{x \in \mathcal{B}_s} e^{\beta \sqrt{2qR'(-b)} \Re\{z^*x\} - \beta R(-b)|x|^2}} Dz dP_s(s) - \frac{b}{\beta}. \quad (42)$$

Moreover, we find

$$\lim_{n \rightarrow 0} \frac{\partial b}{\partial n} = 0. \quad (43)$$

Finally, the fixed point equations (42) and (41) simplify via the saddle point integration rule to (9) and (10). Note that the minimization with respect to the symbol  $x$  splits the integration space of  $z$  into the Voronoi regions defined by the (appropriately scaled) signal constellation  $\mathcal{B}_s$ .

Returning to our initial goal, the evaluation of the average transmitted energy per symbol, and collecting our previous results, we find

$$\begin{aligned}
E_s &= - \lim_{\beta \rightarrow \infty} \frac{1}{\beta} \lim_{n \rightarrow 0} \frac{\partial}{\partial n} \Xi_n \tag{44} \\
&= \lim_{\beta \rightarrow \infty} \frac{1}{\beta} \lim_{n \rightarrow 0} \frac{\partial}{\partial n} (n-1) \int_0^b R(-w) dw + \int_0^{b+\beta nq} R(-w) dw \\
&\quad - \log M(e, f) + \frac{n(n-1)}{2} f^2 \beta^2 q + \frac{n}{2} (f^2 \beta - 2e)(b + \beta q) \\
&= \lim_{\beta \rightarrow \infty} \frac{1}{\beta} \int_0^b R(-w) dw - \frac{b}{\beta} R(-b) + qbR'(-b) - \frac{1}{\beta} \iint \log \sum_{x \in \mathcal{B}_s} e^{\beta f \Re\{z^* x\} - \beta e |x|^2} Dz dP_s(s). \tag{45}
\end{aligned}$$

Now, we use l'Hospital's rule, re-substitute  $b$  and  $q$ , make use of  $b < \infty$  and get (11). Note that for any bound on the amplitude of the signal set  $\mathcal{B}$ , the parameter  $q$  is finite. Even without bound,  $q$  will remain finite for a well-defined minimization problem. The parameter  $b$  behaves in a more complicated manner. It can be both zero, finite, and infinite as  $\beta \rightarrow \infty$  depending on the particular R-transform and the signal sets  $\mathcal{B}_s$ . For  $\beta \notin (0, \infty)$ , the saddle-point limits have to be re-considered.

## V. PARTICULAR RESULTS

The general result leaves us with two components to specify: 1) The statistics of the random matrix entering the energy per symbol via its R-transform. 2) The relaxed signal alphabets  $\mathcal{B}_s \forall s \in \mathcal{S}$ . While the relaxed alphabets characterize a particular method of precoding, the random matrix statistics depends on the wireless communication system. In the following, we will consider the following choice for the statistics of the random matrix.

Consider a vector-valued communication system. Let the received vector be given as

$$\mathbf{r} = \mathbf{H}\mathbf{t} + \mathbf{n} \tag{46}$$

where  $\mathbf{n}$  is white Gaussian noise. Let the components of the transmitted and received vectors be signals sent and received at different antenna elements, respectively.

We want to ensure that the received signal is (up to additive noise) identical to the data vector. This design criteria leads us to choose the precoding matrix

$$\mathbf{T} = \mathbf{H}^\dagger (\mathbf{H}\mathbf{H}^\dagger)^{-1}. \tag{47}$$

This means that we invert the channel and get  $\mathbf{r} = \mathbf{x} + \mathbf{n}$  if the matrix inverse exists. This allows to keep the signal processing at the receiver at a minimum. This is advantageous if the receiver shall be a low-cost or battery-powered device.

To model the statistics of the entries of  $\mathbf{H}$  is a non-trivial task and a topic of ongoing research, see e.g. [2] and references therein. For sake of convenience, we choose in this first order approach that the entries of the channel matrix  $\mathbf{H}$  are independent and identically distributed complex Gaussian random variables with zero mean and variance  $1/N$ . For that case, we find in the appendix that

$$R(w) = \frac{1 - \alpha - \sqrt{(1 - \alpha)^2 - 4\alpha w}}{2\alpha w} \tag{48}$$

$$R'(w) = \frac{\left(1 - \alpha - \sqrt{(1 - \alpha)^2 - 4\alpha w}\right)^2}{4\alpha w^2 \sqrt{(1 - \alpha)^2 - 4\alpha w}}. \tag{49}$$



It also turns out helpful to recognize that

$$\frac{R^2(w)}{R'(w)} = \frac{\sqrt{(1-\alpha)^2 - 4\alpha w}}{\alpha}. \quad (50)$$

In the following, we compare the performances of several constructions of the redundant signal representations for the channel model specified above.

#### A. 1-Dimensional Lattice

Consider binary one-dimensional modulation. Let

$$\mathcal{S} = \{0, 1\} \quad (51)$$

$$\mathcal{B}_1 = -\mathcal{B}_0 \subset \mathbb{R}. \quad (52)$$

This is the mathematical description of binary phase-shift keying on the real line in context of vector precoding.

Using the specifications above, we find in the limit  $\beta \rightarrow \infty$

$$q = \int_{\mathbb{R}} \left| \operatorname{argmin}_{x \in \mathcal{B}_1} \left| z \sqrt{\frac{qR'(-b)}{2R^2(-b)}} - x \right| \right|^2 \frac{e^{-\frac{z^2}{2}} dz}{\sqrt{2\pi}} \quad (53)$$

$$b = \int_{\mathbb{R}} \operatorname{argmin}_{x \in \mathcal{B}_1} \left| z \sqrt{\frac{qR'(-b)}{2R^2(-b)}} - x \right| \frac{z e^{-\frac{z^2}{2}} dz}{\sqrt{4\pi qR'(-b)}}. \quad (54)$$

Moreover, let without loss of generality  $-\infty = c_0 < c_1 < \dots < c_L < c_{L+1} = +\infty$  and

$$\mathcal{B}_1 = \{c_1, c_2, \dots, c_L\} \quad (55)$$

This case describes Tomlinson-Harashima precoding [19], [7] with optimization over  $L$  different representations for each information bit. An example of such a resrepresentation for integer lattice points is shown in Fig. 1. The boundary points of the Voronoi regions are

$$v_i = \frac{c_i + c_{i-1}}{2} \quad (56)$$

and the fixed-point equations for  $q$  and  $b$  become

$$q = \frac{1}{\sqrt{2\pi}} \sum_{i=1}^L \int_{\frac{\sqrt{2}R(-b)v_i}{\sqrt{qR'(-b)}}}^{\frac{\sqrt{2}R(-b)v_{i+1}}{\sqrt{qR'(-b)}}} c_i^2 e^{-\frac{z^2}{2}} dz \quad (57)$$

$$= c_1^2 + \sum_{i=2}^L (c_i^2 - c_{i-1}^2) Q \left( \frac{R(-b)(c_i + c_{i-1})}{\sqrt{2qR'(-b)}} \right) \quad (58)$$

$$b = \frac{\sum_{i=2}^L (c_i - c_{i-1}) \exp \left( -\frac{R^2(-b)(c_i + c_{i-1})^2}{4qR'(-b)} \right)}{\sqrt{4\pi qR'(-b)}} \quad (59)$$

with  $Q = \int_x^\infty \exp(-x^2/2) dx / \sqrt{2\pi}$  denoting the Gaussian probability integral.

For the case of no precoding at all, i.e.  $L = 1$ , we get

$$b = 0 \quad (60)$$

$$q = c_1^2 \quad (61)$$

$$E_s = c_1^2 R(0). \quad (62)$$

For the case of general  $L$ , we first restrict to the special case of a square channel matrix. The rectangular case is addressed subsequently.

1) *Square Channel Matrix*: For  $\alpha = 1$ , (48) and (49) respectively simplify to

$$R(w) = \frac{1}{\sqrt{-w}} \quad (63)$$

$$R'(w) = \frac{1}{2(-w)^{\frac{3}{2}}}. \quad (64)$$

Thus, we find

$$E_s \rightarrow \infty \quad \text{if } \lim_{\beta \rightarrow \infty} b = 0. \quad (65)$$

For positive values of  $b$ , we get

$$q = c_1^2 + \sum_{i=2}^L (c_i^2 - c_{i-1}^2) Q\left(b^{\frac{1}{4}} q^{-\frac{1}{2}} (c_i + c_{i-1})\right) \quad (66)$$

$$b = \frac{b^{\frac{3}{4}}}{\sqrt{2\pi q}} \sum_{i=2}^L (c_i - c_{i-1}) \exp\left(-\frac{\sqrt{b}(c_i + c_{i-1})^2}{2q}\right). \quad (67)$$

and

$$E_s = \frac{q}{2\sqrt{b}} \quad (68)$$

which makes the case distinction with respect to the asymptotic behavior of  $b$  obsolete. Moreover, we can combine the above 3 equations to find

$$E_s = \pi \left[ \frac{c_1^2 + \sum_{i=2}^L (c_i^2 - c_{i-1}^2) Q\left(\frac{c_i + c_{i-1}}{\sqrt{2E_s}}\right)}{\sum_{i=2}^L (c_i - c_{i-1}) \exp\left(-\frac{(c_i + c_{i-1})^2}{4E_s}\right)} \right]^2. \quad (69)$$

Numerical solutions to (69) are shown in Table I for the equally spaced integer lattice

$$\mathcal{B}_0 = \{+1, -3, +5, -7, +9, \dots\} \quad (70)$$

and various numbers of lattice points. Obviously, there is little improvement when going from two to three lattice points and negligible improvement for more than 3 lattice points.

2) *Rectangular Channel Matrix*: For a rectangular channel matrix, the Gramian is only invertible for  $\alpha \leq 1$ . However, the R-transform is well-defined for any positive aspect ratio. For singular random matrices, the R-transform reflects the fact that the asymptotic eigenvalue distribution has some point mass at infinity.

Thus, we find

$$q = c_1^2 + \sum_{i=2}^L (c_i^2 - c_{i-1}^2) Q\left(\frac{((1-\alpha)^2 + 4\alpha b)^{\frac{1}{4}} (c_i + c_{i-1})}{\sqrt{2q\alpha}}\right)$$

$$b = \frac{b\sqrt{\frac{\alpha}{\pi q} \sqrt{(1-\alpha)^2 + 4\alpha b}}}{\alpha - 1 + \sqrt{(1-\alpha)^2 + 4\alpha b}} \sum_{i=2}^L (c_i - c_{i-1}) e^{-\frac{\sqrt{(1-\alpha)^2 + 4\alpha b} (c_i + c_{i-1})^2}{4q\alpha}}.$$

It is convenient to replace the parameter  $b$  by the substitution

$$p = \sqrt{(1-\alpha)^2 + 4\alpha b} \quad (71)$$

which gives

$$q = c_1^2 + \sum_{i=2}^L (c_i^2 - c_{i-1}^2) Q \left( \sqrt{\frac{p}{2q\alpha}} (c_i + c_{i-1}) \right)$$

$$p = 1 - \alpha + \sqrt{\frac{\alpha p}{\pi q}} \sum_{i=2}^L (c_i - c_{i-1}) \exp \left( -\frac{p(c_i + c_{i-1})^2}{4q\alpha} \right)$$

and

$$E_s = \frac{q}{p}. \quad (72)$$

Finally, combining the last three equations, we get

$$E_s = \frac{c_1^2 + \sum_{i=2}^L (c_i^2 - c_{i-1}^2) Q \left( \frac{c_i + c_{i-1}}{\sqrt{2\alpha E_s}} \right)}{1 - \alpha + \sqrt{\frac{\alpha}{\pi E_s}} \sum_{i=2}^L (c_i - c_{i-1}) \exp \left( -\frac{(c_i + c_{i-1})^2}{4\alpha E_s} \right)} \quad (73)$$

The solutions of these fixed-point equations are shown by the solid lines in Fig. 2. Clearly for small load, the parameter  $q$  tends to 1, i.e. 0 dB, as in that case, no gain due to precoding is possible and the symbol with smallest magnitude is preferred. The minimum of the transmit power is shown by the solid line in Fig. 3. Note that precoding enables to achieved finite transmitted energy per symbol even if the channel matrix is singular. This effect has already been explained for Marchenko-Pastur distributed random matrices. Unlike the curve without precoding, the curves for  $L > 1$  do not have poles at the threshold load. Instead, a phase transition occurs and the energy per symbol jumps discontinuously from a finite value to infinity. In fact, it can be shown that the threshold load at which this happens is universal for a large class of random matrices in that it depends only on the specifics of the precoding lattice but not on the channel statistics.

## B. 2-Dimensional Quadrature Lattice

Consider now the case shown in Fig. 4. It has the following properties:

$$\mathcal{S} = \{00, 01, 10, 11\} \quad (74)$$

$$\mathcal{B}_{1y} = -\mathcal{B}_{0y}^* \quad \forall y \in \{0, 1\} \quad (75)$$

$$\mathcal{B}_{x1} = +\mathcal{B}_{x0}^* \quad \forall x \in \{0, 1\} \quad (76)$$

This case extends the one-dimensional precoding of binary phase-shift keying (BPSK) on the real line to two-dimensional precoding of quaternary phase-shift keying (QPSK) in the complex plane such that Gray mapping is applied and we can consider the pre-coding for QPSK as independent pre-coding of BPSK in both quadrature components.

The symmetry in both quadrature components implies that

$$q = \sqrt{\frac{2}{\pi}} \int_{\mathbb{R}} \left| \operatorname{argmin}_{x \in \mathbb{R}\{\mathcal{B}_{1+j}\}} \left| z \sqrt{\frac{qR'(-b)}{2R^2(-b)}} - x \right| \right|^2 e^{-\frac{z^2}{2}} dz \quad (77)$$

$$b = \int_{\mathbb{R}} \operatorname{argmin}_{x \in \mathbb{R}\{\mathcal{B}_{1+j}\}} \left| z \sqrt{\frac{qR'(-b)}{2R^2(-b)}} - x \right| \frac{z e^{-\frac{z^2}{2}} dz}{\sqrt{\pi q R'(-b)}}. \quad (78)$$

Compared to the one-dimensional case, the only difference is that the right hand sides of the two fixed point equations are multiplied by a factor of 2 which stems from adding the contributions of both quadrature

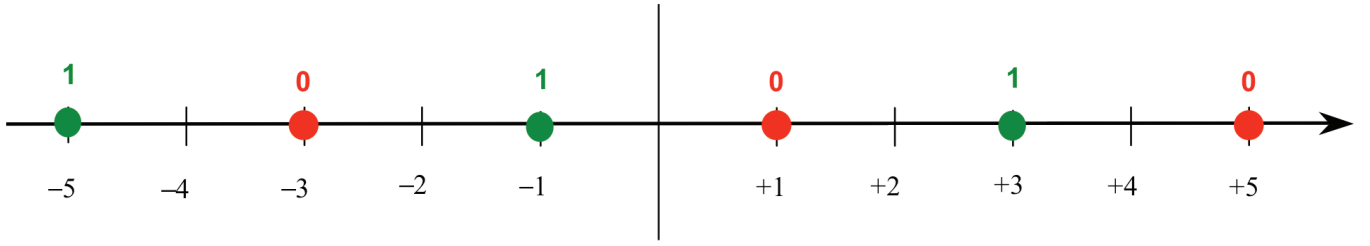


Fig. 1. 2 one-dimensional equally spaced integer lattices representing the two binary states 0 and 1, respectively.

TABLE I  
ENERGY PER SYMBOL FOR INVERTED SQUARE CHANNEL.

$L$	1	2	3	4	$\infty$
$E_s$	$\infty$	2.6942	2.6656	2.6655	2.6655
$E_s$ [dB]	$\infty$	4.3043	4.2579	4.2578	4.2578

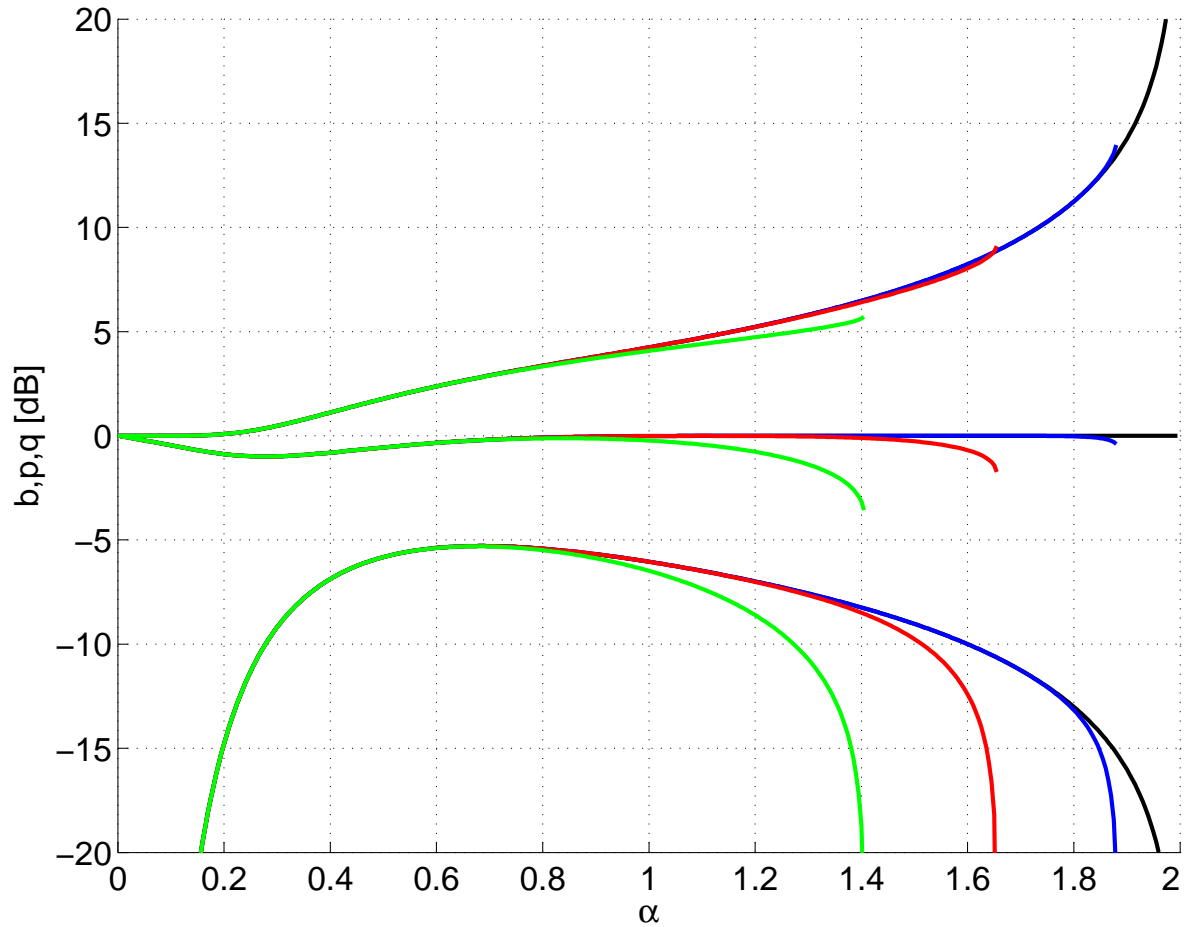


Fig. 2. The macroscopic parameters  $q$  (upper lines),  $b$  (lower lines), and  $p$  (medium lines) versus the load  $\alpha$  for  $L = 2, 3, 6, 100$ . shown by green, red, blue, and black lines, respectively.

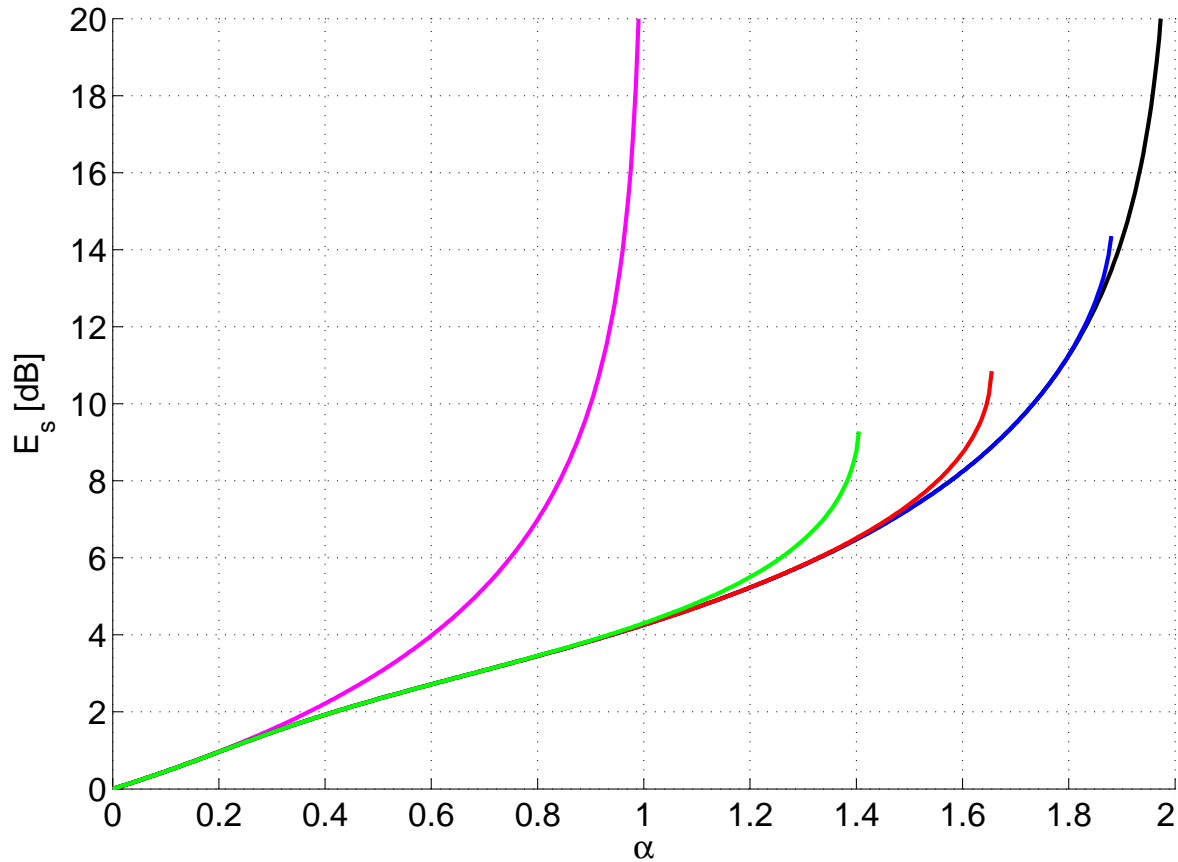


Fig. 3. The transmitted energy per symbol versus the load for  $L = 1, 2, 3, 6, 100$  shown by the magenta, green, red, blue, and black lines, respectively.

components. In order to allow for a fair comparison with 1-dimensional modulation, we shall consider the energy per bit

$$E_b = \frac{E_s}{\log_2 |\mathcal{S}|} \quad (79)$$

to be the performance measure of choice.

Due to de-coupling between quadrature components, we find that (72) remains valid and  $p$  and  $q$  are given by

$$q = 2c_1^2 + 2 \sum_{i=2}^L (c_i^2 - c_{i-1}^2) Q \left( \sqrt{\frac{p}{2q\alpha}} (c_i + c_{i-1}) \right) \quad (80)$$

$$p = 1 - \alpha + \sqrt{\frac{4\alpha p}{\pi q}} \sum_{i=2}^L (c_i - c_{i-1}) e^{-\frac{p(c_i + c_{i-1})^2}{4q\alpha}}. \quad (81)$$

The solutions to these fixed point equations are shown in Fig. 5. Remarkably, the energy per bit remains as small as  $E_b = \frac{4}{3}$  for any load if  $L$  grows large.

### C. 2-Dimensional Checkerboard Lattice

Consider now the case shown in Fig. 6. This case extends the one-dimensional pre-coding of BPSK

on the real line to two-dimensional pre-coding of BPSK in the complex plane. Among others, it has the following properties:

$$\mathcal{S} = \{0, 1\} \quad (82)$$

$$\mathcal{B}_1 = j\mathcal{B}_0 \subset \mathbb{C}. \quad (83)$$

This mapping is like a checkerboard where the sets  $\mathcal{B}_1$  and  $\mathcal{B}_0$  correspond to the black and white fields, respectively. For this mapping, the boarderlines of the Voronoi regions are not parallel to the real and imaginary axes but intersect these by an angle of  $45^\circ$ .

Considering an unconstrained lattice, i.e. infinitely many lattice points, we can rotate the lattice by  $45^\circ$  degrees without loss of generality due to the rotational invariance of the complex Gaussian integral kernel in the fixed-point equations for  $b$  and  $q$ . After rotation we find the same lattice as in the two-dimensional quadrature precoding except for a lattice scaling by a factor of  $1/\sqrt{2}$ . Thus, the energy per symbol will be half the energy per symbol of quadrature precoding and the energy per bit will be identical.

#### D. 2-Dimensional Semi-Discrete Lattice

Consider now the case shown in Fig. 7. This mapping is identical to the 1-dimensional lattice except for the fact that the imaginary parts of the symbols in  $\mathcal{B}_x$  are left arbitrary.

This mapping has the following properties

$$\mathcal{S} = \{0, 1\} \quad (84)$$

$$\mathcal{B}_1 = -\mathcal{B}_0 \subset \mathbb{C} \quad (85)$$

which lead to

$$q = \frac{qR'(-b)}{2R^2(-b)} + \int_{\mathbb{R}} \left| \operatorname{argmin}_{x \in \mathcal{R}\{\mathcal{B}_1\}} \left| z \sqrt{\frac{qR'(-b)}{2R^2(-b)}} - x \right| \right|^2 \frac{e^{-\frac{z^2}{2}} dz}{\sqrt{2\pi}} \quad (86)$$

$$b = \frac{1}{2R(-b)} + \int_{\mathbb{R}} \operatorname{argmin}_{x \in \mathcal{R}\{\mathcal{B}_1\}} \left| z \sqrt{\frac{qR'(-b)}{2R(-b)^2}} - x \right| \frac{z e^{-\frac{z^2}{2}} dz}{\sqrt{4\pi q R'(-b)}}. \quad (87)$$

For channel inversion, we have

$$\frac{R'(-b)}{R^2(-b)} = \frac{\alpha}{p}. \quad (88)$$

This enables us to easily solve the fixed point equations.

Fig. 8 compares the complex semi-discrete lattice with the complex quadrature lattice in terms of energy per bit. Precoding with semi-discrete lattices achieves a remarkable gain which comes at the expense of reduced data rate. It is particularly worth to remark that the semi-discrete lattice with  $L = 1$  outperforms all quadrature lattices for loads up to  $\alpha \approx 0.479$ . Note that for  $L = 1$ , the sets  $\mathcal{B}_s$  are convex. Thus, the quadratic programming problem is convex since  $\mathbf{J}$  is positive semidefinite and it can be solved with a polynomial time algorithm [1]. For large loads and large lattice size, the energy per bit approaches  $E_b = \frac{4}{3}$ .

## VI. CONCLUSIONS

We have found that vector pre-coding can significantly reduce the required transmitted power. In fact, with appropriate pre-coding, the transmitted power stays always finite. Moreover, we found strong advantages of complex-valued pre-coding over real-valued pre-coding and a trade-off between data rate and required transmit power.

We are aware of the fact that replica symmetry might not hold. Therefore, we have started investigating first order replica symmetry breaking (1RSB). The quantitative analysis is not finished yet, but qualitatively, the results remain unchanged for 1RSB.

## ACKNOWLEDGMENTS

This research was supported by the Research Council of Norway, the National Science Foundation, DARPA, and the European Commission under grants 171133/V30, CCF-0644344, W911NF-07-1-0028, and MIRG-CT-2005-030833, resp. It was initiated while R. Müller and D. Guo were visiting the Institute for Mathematical Sciences at the National University of Singapore in 2006.

## APPENDIX

Let  $p_X(x)$  be an arbitrary pdf such that both the Stieltjes transform defined in (4) and

$$m_{X^{-1}}(s) = \int \frac{dP_X(x)}{\frac{1}{x} - s} \quad (89)$$

exist for some complex  $s$  with  $\Im(s) > 0$ . It can easily be checked that

$$m_{X^{-1}}\left(\frac{1}{s}\right) = -s(1 + sm_X(s)). \quad (90)$$

Let  $s = m_X^{-1}(-w)$ . Then, we find

$$m_{X^{-1}}\left(\frac{1}{m_X^{-1}(-w)}\right) = -m_X^{-1}(-w)(1 - wm_X^{-1}(-w)). \quad (91)$$

and

$$\frac{1}{m_X^{-1}(-w)} = m_{X^{-1}}^{-1}(-m_X^{-1}(-w)(1 - wm_X^{-1}(-w))). \quad (92)$$

With Definition 1, we find

$$\frac{1}{R_X(w) + \frac{1}{w}} = R_{X^{-1}}\left(-wR_X(w)\left(R_X(w) + \frac{1}{w}\right)\right) - \frac{1}{wR_X(w)\left(R_X(w) + \frac{1}{w}\right)} \quad (93)$$

and

$$\frac{1}{R_X(w)} = R_{X^{-1}}(-R_X(w)(1 + wR_X(w))). \quad (94)$$

It is well known [21], [20] that for an  $N \times \alpha N$  random matrix  $\mathbf{H}$  with i.i.d. entries of variance  $(\alpha N)^{-1}$ , the R-transform of the limiting spectral measure  $P_{\mathbf{H}^\dagger \mathbf{H}}(x)$  is given by

$$R_{\mathbf{H}^\dagger \mathbf{H}}(w) = \frac{1}{1 - \alpha w}. \quad (95)$$

Letting  $X^{-1} = \mathbf{H}^\dagger \mathbf{H}$ , we find

$$R_{(\mathbf{H}^\dagger \mathbf{H})^{-1}}(w) = 1 + \alpha R_{(\mathbf{H}^\dagger \mathbf{H})^{-1}}(w) \left(1 + wR_{(\mathbf{H}^\dagger \mathbf{H})^{-1}}(w)\right) \quad (96)$$

with (94). Solving (96) for the R-transform implies (48). Note that for  $\alpha \geq 1$ , the mean of the spectral measure is diverging. Thus, the R-transform must have a pole at  $w = 0$  which excludes the other solution of (96).

## REFERENCES

- [1] S. P. Boyd and L. Vandenberghe. *Convex Optimization*. Cambridge University Press, 2004.
- [2] M. Debbah and R. Müller. MIMO channel modelling and the principle of maximum entropy. *IEEE Transactions on Information Theory*, 51(5):1667–1690, May 2005.
- [3] K. Fischer and J. Hertz. *Spin Glasses*. Cambridge University Press, Cambridge, U.K., 1991.
- [4] R. F. Fischer. *Precoding and Signal Shaping for Digital Transmission*. John Wiley & Sons, 2002.
- [5] G. Foschini and M. Gans. On limits of wireless communications in a fading environment when using multiple antennas. *Wireless Personal Communications*, 6:311–335, 1998.
- [6] A. Guionnet and M. Maïda. A Fourier view on the R-transform and related asymptotics of spherical integrals. *Journal of Functional Analysis*, 222:435–490, 2005.
- [7] H. Harashima and H. Miyakawa. Matched-transmission technique for channels with intersymbol interference. *IEEE Transactions on Communications*, COM-20:774–780, Aug. 1972.
- [8] . Harish-Chandra. Fourier transforms on a semisimple Lie algebra I. *American Journal of Mathematics*, 79:193–257, 1957.
- [9] B. M. Hochwald, C. Peel, and A. Swindlehurst. A vector-perturbation technique for near-capacity multiantenna multiuser communication-Part II: Perturbation. *IEEE Transactions on Communications*, 53(3):537–544, Mar. 2005.
- [10] C. Itzykson and J. Zuber. The planar approximation (II). *Journal of Mathematical Physics*, 21(3):411–421, Mar. 1980.
- [11] S. Kirkpatrick and D. Sherrington. Infinite-ranged models of spin-glasses. *Physics Review B*, 17(11), 1978.
- [12] E. Marinari, G. Parisi, and F. Ritort. Replica field theory for deterministic models (II): A non-random spin glass with glassy behavior. *Journal of Physics A: Math. & Gen.*, 27:7647–7668, 1994.
- [13] M. Mezard, G. Parisi, and M. A. Virasoro. *Spin Glass Theory and Beyond*. World Scientific, Singapore, 1987.
- [14] H. Nishimori. *Statistical Physics of Spin Glasses and Information Processing*. Oxford University Press, Oxford, U.K., 2001.
- [15] G. Parisi. A sequence of approximated solutions to the S-K model for spin glasses. *Journal of Physics A: Math. & Gen.*, 13, 1980.
- [16] C. B. Peel, B. M. Hochwald, and A. L. Swindlehurst. A vector-perturbation technique for near-capacity multiantenna multiuser communication-Part I: Channel inversion and regularization. *IEEE Transactions on Communications*, 53(1):195–202, Jan. 2005.
- [17] K. Takeda, S. Uda, and Y. Kabashima. Analysis of CDMA systems that are characterized by eigenvalue spectrum. *Europhysics Letters*, 76(6):1193–1199, 2006.
- [18] I. E. Telatar. Capacity of multi-antenna Gaussian channels. *European Trans. Telecommunications*, 10(6):585–595, Nov./Dec. 1999.
- [19] M. Tomlinson. New automatic equaliser employing modulo arithmetic. *IEE Electronics Letters*, 7:138–139, Mar. 1971.
- [20] A. M. Tulino and S. Verdú. Random matrix theory and wireless communications. *Foundations and Trends in Communications and Information Theory*, 1(1), June 2004.
- [21] D. V. Voiculescu, K. J. Dykema, and A. Nica. *Free Random Variables*. American Mathematical Society, Providence, RI, 1992.
- [22] B. R. Vojčić and W. M. Jang. Transmitter precoding in synchronous multiuser communications. *IEEE Transactions on Communications*, 46(10):1346–1355, Oct. 1998.
- [23] C. Windpassinger, R. F. H. Fischer, T. Vencel, and J. B. Huber. Precoding in multiantenna and multiuser communications. *IEEE Transactions on Wireless Communications*, 3(4):1305–1316, July 2004.



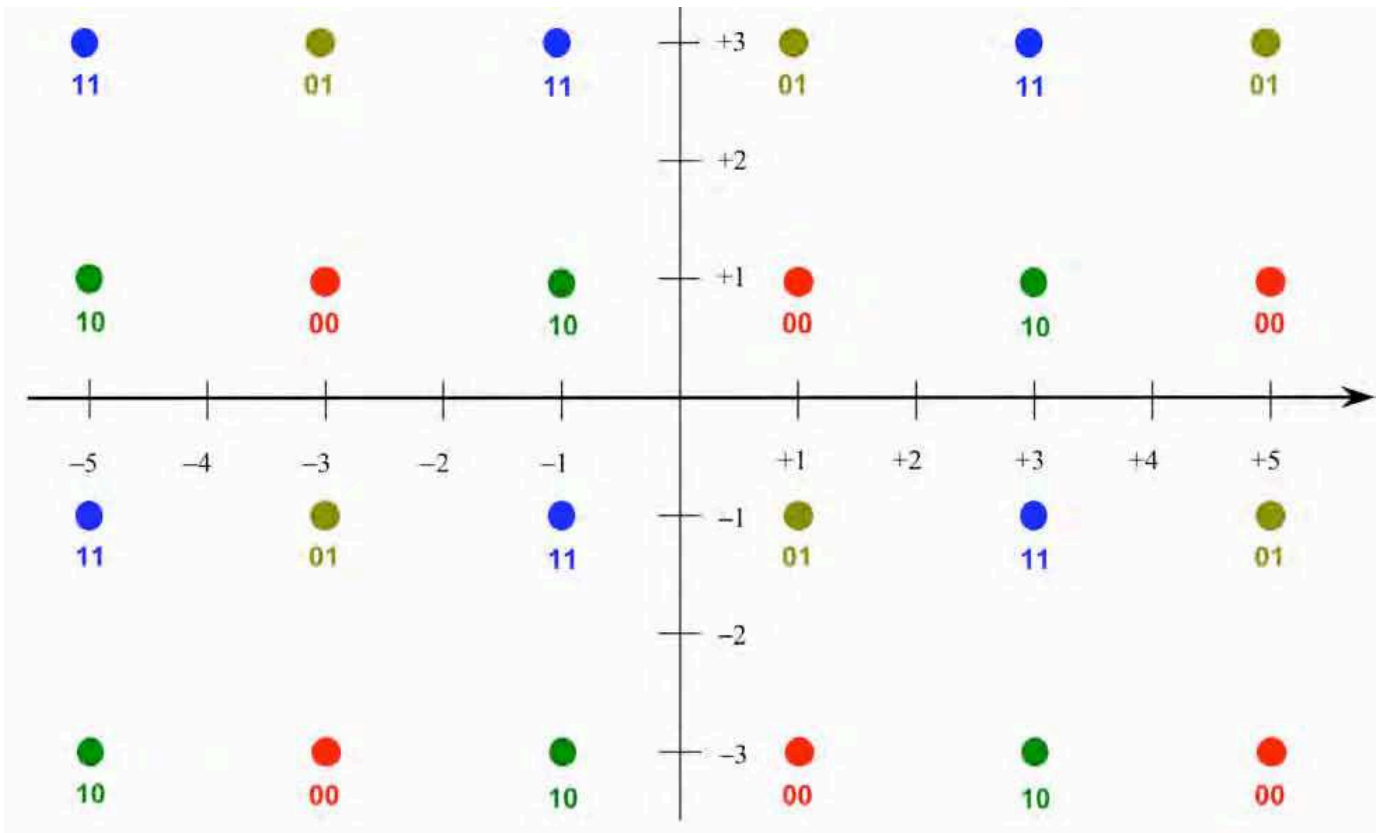


Fig. 4. 4 two-dimensional equally spaced integer quadrature lattices representing the four quaternary states 00, 01, 10, and 11, respectively.

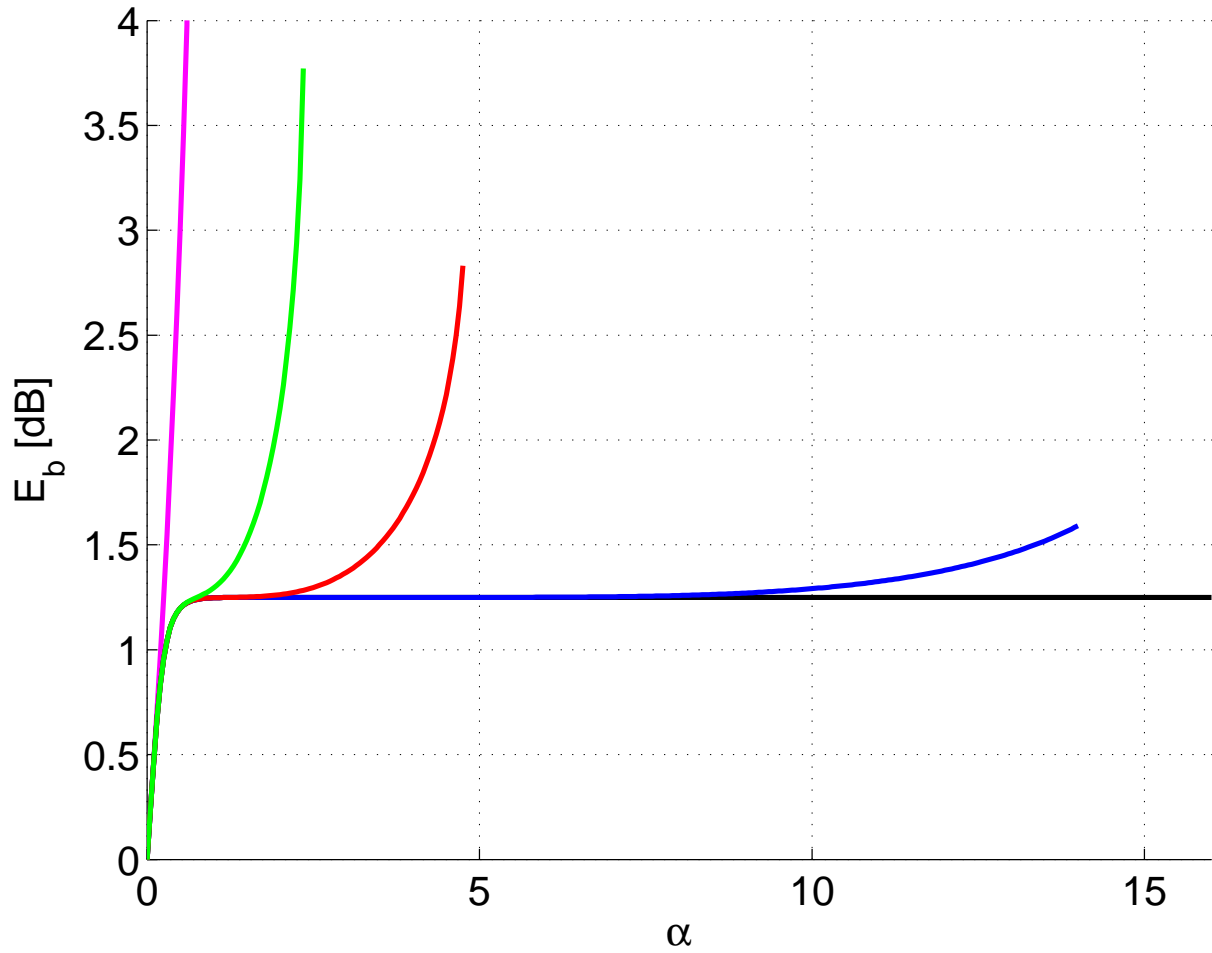


Fig. 5. Transmitted energy per bit versus the load for channel inversion and pre-coding for Gray-mapped QPSK with  $L = 1, 2, 3, 6, 100$  shown by the magenta, green, blue, and black lines respectively.

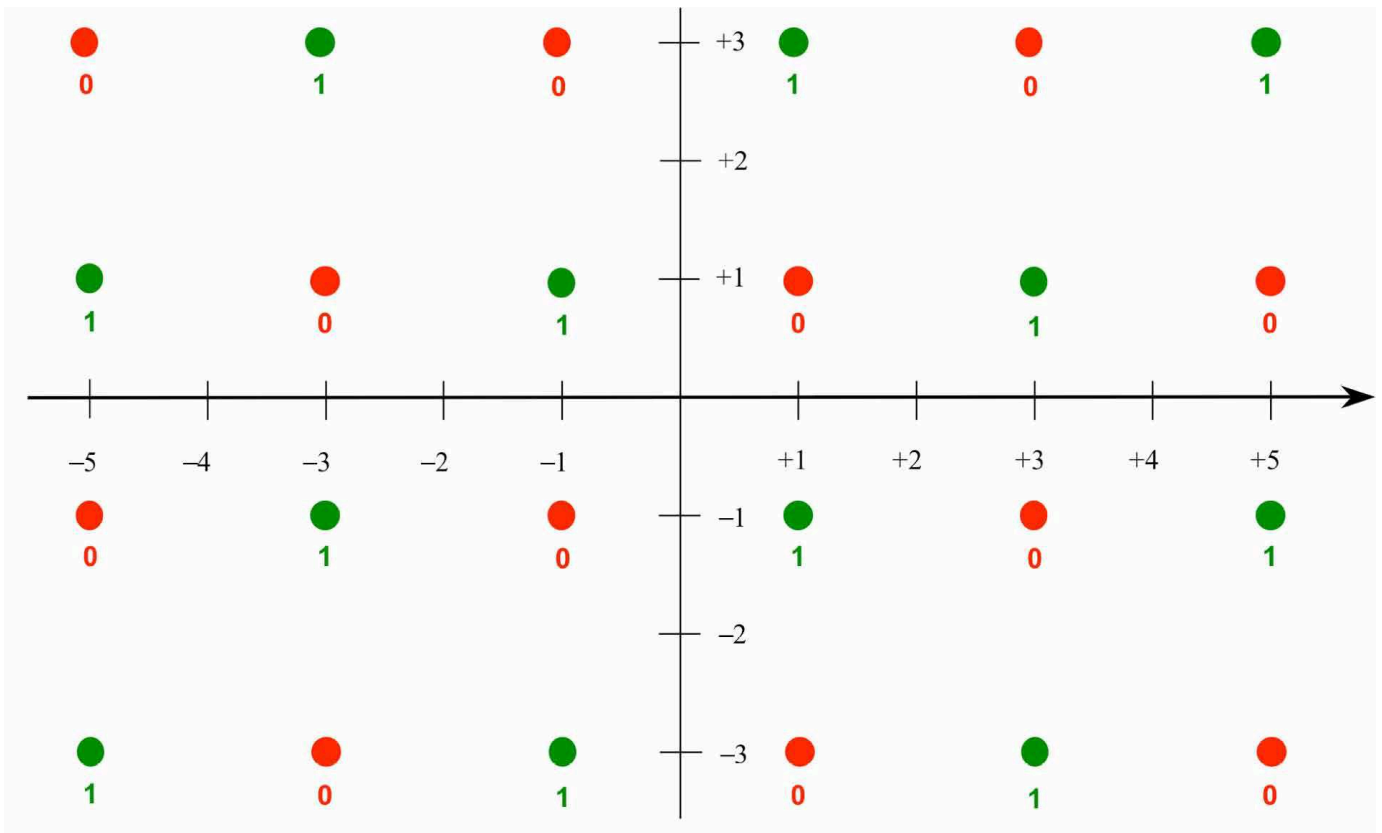


Fig. 6. 2 two-dimensional equally spaced integer quadrature lattices representing the two binary states 0 and 1, respectively.

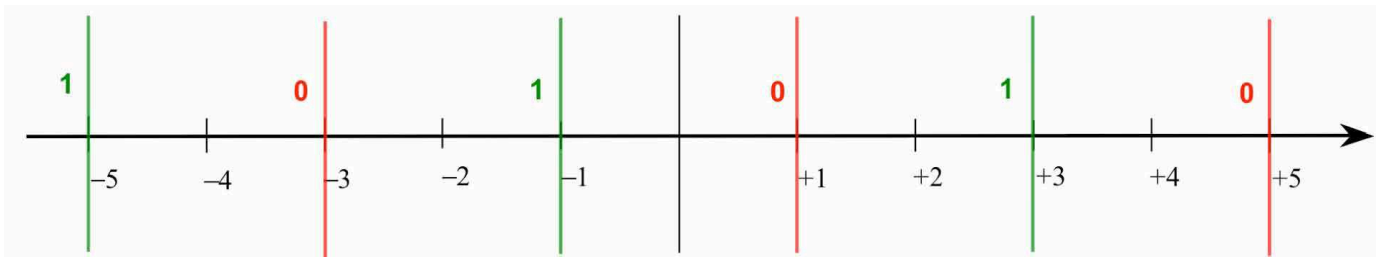


Fig. 7. 2 two-dimensional equally spaced semi-discrete lattices representing the two binary states 0 and 1, respectively.

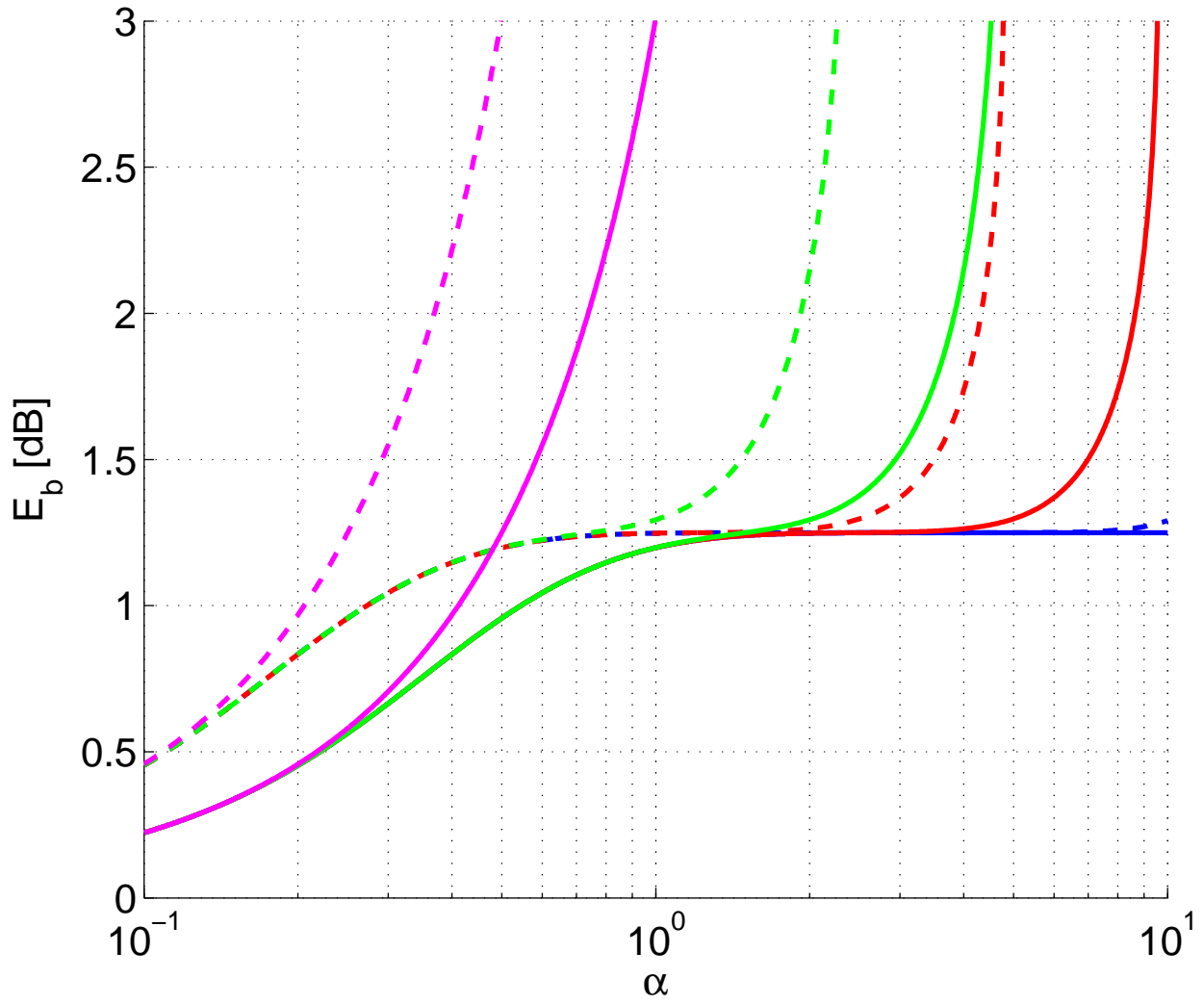


Fig. 8. Energy per bit versus load for precoding with complex quadrature lattice (dashed lines) and semi-discrete lattice (solid lines) for  $L = 1, 2, 3, 6$  shown by the magenta, green, red, and blue lines, respectively.